Journal of Control, Automation and Electrical Systems (2018) 29:177–191
https://doi.org/10.1007/s40313-017-0362-7

Optimal Power Flow For Multi-FACTS Power System Using Hybrid PSO-PS Algorithms

Fateh Berrouk[1] · **Kamel Bounaya**[1]

Received: 2 May 2017 / Revised: 13 December 2017 / Accepted: 28 December 2017 / Published online: 9 January 2018
© Brazilian Society for Automatics–SBA 2018

Abstract
This paper presents an efficient hybrid particle swarm optimization and pattern search algorithms for the solution of optimal power flow problem with inclusion of flexible AC transmission systems (FACTS) devices. The purpose of the proposed technique is to merge the advantages of both PSO in exploitation and PS in exploration to achieve the best solution. The FACTS devices considered in this study are thyristor-controlled series compensator and static var compensator. These devices aim to minimize the total generation cost, enhance voltage deviation, decrease real and reactive losses and improve the voltage stability index. The proposed method is carried out on the standard IEEE 30-bus system, and obtained results are compared to other methods reported in the literature. Simulation results demonstrate the effectiveness and potential of the proposed method.

Keywords Optimal power flow · Voltage stability · Power losses · Particle swarm optimization · Pattern search · FACTS

1 Introduction

The optimal power flow (OPF) problem, which was proposed for the first time by Carpentier (1962) and developed by Dommel and Tinney (1968), is the major concern for considerable research work in power system operation and planning domain. The aim of the optimal power flow is to optimize a chosen objective function like fuel cost by determining the optimal combination of real power generation, voltage of generators, reactive power injection and transformer tap position, while at the same time satisfying a set of physical and operational constraints, which are imposed by equipment and network limitations (Niknam et al. 2011).

Generally, OPF is a large-scale, nonconvex and nonlinear optimization problem with a large number of variables (Mahdad and Srairi 2014). Earlier, several mathematical programming-based techniques have been proposed to solve the OPF problem. The most popular are linear programming (LP) (Al-Muhawesh and Qamber 2008), quadratic programming (QP) (Momoh et al. 1994), the interior point method (IPM) (Momoh and Zhu 1999) and Newton method (NM) (Sun et al. 1984). Unfortunately, these classical methods suffer from many drawbacks, such as being converged to local optimal, and do not guarantee finding the global one, resulting in huge computations and large execution time, and finally these methods, which are based on gradients and derivatives, are highly complex and inefficient for large-scale system applications (Daryani et al. 2016).

Recently, various population-based optimization techniques, such as genetic algorithm (GA) (Bouktir et al. 2004), particle swarm optimization (PSO) (Abido 2002a), artificial bee colony (ABC) (Ayan et al. 2015), black-hole-based optimization (BHBO) (Bouchekara 2014), differential evolution (DE) (Abou El Ela and Abido 2010), electromagnetism-like mechanism algorithm (EM) (Bouchekara 2016), simulated annealing (SA) (Roa-Sepulveda and Pavez-Lazo 2003), tabu search (TS) (Abido 2002b), have been successfully used to solve the OPF problems. Unlike many conventional algorithms, these methods are proved by their efficiency in identification of global optimum.

Furthermore, several hybrid optimization techniques have been developed and successfully used to solve OPF problem. These methods are robust and powerful in terms of fast convergence and in finding the global optimum. Some of these techniques are hybrid differential evolution (DE) with particle swarm optimization (PSO) (Gnanambal and Babulal 2012), hybrid PSO and simulated annealing (SA)

✉ Fateh Berrouk
fateh.ber@gmail.com

[1] Electrical Engineering Laboratory, 08 May 1945 University, 24000 Guelma, Algeria

(Niknam et al. 2012b), new hybrid algorithm named DE–APSO–PS consisting of DE, adaptive PSO and pattern search (PS) (Mahdad and Srairi 2014), a novel hybrid algorithm of imperialist competitive algorithm (ICA) and teaching learning algorithm (TLA) (Ghasemi et al. 2014b), hybrid PSO with an aging leader and challengers algorithm (ALC) (Singh et al. 2016), hybrid fuzzy PSO and Nelder–Mead algorithm (HFPSO–NM) (Joorabian and Afzalan 2014), hybrid tabu search and simulated annealing algorithm TS/SA (Ongsakul and Bhasaputra 2002).

On the other hand, FACTS devices represent an efficiency tool which was extensively used to improve the performances of overall power system by controlling power flow through transmission lines and voltage profile. These devices are introduced in OPF problem for various objectives such as total fuel cost reduction in Ongsakul and Bhasaputra (2002) and Mahdad et al. (2010), real power losses and emission minimization in Basu (2011) and Mukherjee and Mukherjee (2016), voltage deviation enhancement in Mahdad and Srairi (2014) and Abarghooeea et al. (2014) and voltage stability improvement in (Abarghooeea et al. 2014; Mahdad and Srairi 2015).

The aim of the present paper is, firstly, to demonstrate the effectiveness of the proposed PSO-PS algorithm to solve the OPF problem of power system equipped with FACTS devices, and secondly, two kinds of FACTS devices are proposed to improve the solution of OPF problems for different objectives. Thyristor-controlled series compensator (TCSC) and static var compensator (SVC) are considered here in aim to reduce generation cost, enhance voltage deviation, decrease real and reactive losses and improve the voltage stability index. The effectiveness of the proposed work is tested on IEEE 30-bus test system. The obtained results are compared to other methods reported in the literature.

The rest of this paper is organized as follows: Sect. 2 describes the formulation of the OPF problem, then, Sect. 3 explains the proposed hybrid PSO-PS algorithm, while Sect. 4 introduces the modeling of TCSC and SVC devices, and Sect. 5 shows numerical results and discussion of the simulation carried out on the 30-bus system, and finally, Sect. 6 presents the conclusion.

2 Optimal Power Flow Problem Formulation

The aim of solving the optimal power flow problem is to optimize a set of control variables in order to minimize a predefined objective function while satisfying equality and inequality constraints. Mathematically, the OPF problem can be formulated as follows (Ghasemi et al. 2014a; Bouchekara et al. 2014):

$$\text{Minimize } F(x,u) \tag{1}$$

$$\text{Subject to } g(x,u)=0 \tag{2}$$

$$\text{And } h(x,u)\le 0 \tag{3}$$

where $F(x,u)$ is the objective function, and $g(x,u)$ and $h(x,u)$ are, respectively, the set of equality and inequality constraints.

u is the set of control variables consisting of active power generation at the PV buses except at the slack P_{G}, voltage magnitude at PV buses V_{G}, tap settings of transformer T, shunt VAR compensation Q_{C}, furthermore, reactance values of TCSC devices X_{TCSC}, and SVC's susceptance B_{SVC}. Accordingly, the u vector can be illustrated as the following:

$$u^T=\begin{bmatrix} P_{\mathrm{G}_2}\dots P_{\mathrm{G}_{\mathrm{NG}}}, V_{\mathrm{G}_1}\dots V_{\mathrm{G}_{\mathrm{NG}}}, Q_{\mathrm{C}_1}\dots Q_{\mathrm{C}_{\mathrm{NC}}}, T_1\dots T_{\mathrm{NT}}, \\ X_{\mathrm{TCSC}_1}\dots X_{\mathrm{TCSC}_{\mathrm{NTCSC}}}, B_{\mathrm{SVC}_1}\dots B_{\mathrm{SVC}_{\mathrm{NSVC}}} \end{bmatrix} \tag{4}$$

where NG, NT, NC, NTCSC, NSVC indexes represent the number of generators, the number of regulating transformers, the number of VAR compensators, the number of TCSC devices and the number of SVC devices, respectively.

x is the set of state variables consisting of active power output at slack bus P_{G1}, voltage magnitude at PQ buses, load buses V_{L}, reactive power output of all generator units Q_{G}, transmission line flow S_l. Accordingly, the x vector can be illustrated as the following:

$$x^T=\left[P_{\mathrm{G}_1}, V_{L_1}\dots V_{L_{\mathrm{NL}}}, Q_{\mathrm{G}_1}\dots Q_{\mathrm{GNG}}, S_{L_1}\dots Sl_{\mathrm{Nl}}\right] \tag{5}$$

where NL and Nl are the number of load buses and the number of transmission lines, respectively.

2.1 Constraints

2.1.1 Equality Constraints

The power flow equations, as the main equality constraint $g(x,u)$, present the physics of the power systems. The general form of power flow equations is as follows (Bouchekara et al. 2014):

$$P_{\mathrm{G}i}-P_{\mathrm{D}i}-V_i\sum_{j=1}^{\mathrm{NB}}V_j\left[G_{ij}\cos\left(\theta_{ij}\right)+B_{ij}\sin\left(\theta_{ij}\right)\right]=0 \tag{6}$$

$$Q_{\mathrm{G}i}-Q_{\mathrm{D}i}-V_i\sum_{j=1}^{\mathrm{NB}}V_j\left[G_{ij}\sin\left(\theta_{ij}\right)+B_{ij}\cos\left(\theta_{ij}\right)\right]=0 \tag{7}$$

where P_{G} is the active power generation, Q_{G} is the reactive power generation, P_{D} is the active demand, Q_{D} is the reactive load demand, V_i and V_j are the voltages of i-th and j-th bus, respectively, NB is the number of buses, G_{ij}, B_{ij} are the real and imaginary parts of the admittance matrix Y_{ij}, representing

the conductance and susceptance between bus i and bus j, respectively.

2.1.2 Inequality Constraints

The inequality constraints $h(x, u)$ of the OPF problem indicate the limits on physical devices of the network which include (Bouchekara 2014):

a. Generator constraints: Generator voltage, active and reactive power of the i-th bus should lie between their respective maximum and minimum limits as follows:

$$V_{G_i}^{\min} \le V_{G_i} \le V_{G_i}^{\max}, \quad i = 1, \ldots, \text{NG} \tag{8}$$

$$P_{G_i}^{\min} \le P_{G_i} \le P_{G_i}^{\max}, \quad i = 1, \ldots, \text{NG} \tag{9}$$

$$Q_{G_i}^{\min} \le Q_{G_i} \le Q_{G_i}^{\max}, \quad i = 1, \ldots, \text{NG} \tag{10}$$

b. Transformer tap constraints: Transformer tap settings must be bounded between maximum and minimum limits as follows:

$$T_i^{\min} \le T_i \le T_i^{\max}, \quad i = 1, \ldots, \text{NT} \tag{11}$$

c. Shunt compensator constraints: Shunt compensations must be restricted by their maximum and minimum limits as follows:

$$Q_{C_i}^{\min} \le Q_{GC_i} \le Q_{C_i}^{\max}, i = 1, \ldots, \text{NG} \tag{12}$$

d. Security constraints: Include the constraints of voltages at load buses and transmission line loading as follows:

$$V_{L_i}^{\min} \le V_{L_i} \le V_{L_i}^{\max}, \quad i = 1, \ldots, \text{NL} \tag{13}$$

$$S_{l_i} \le S_{l_i}^{\max}, \quad i = 1, \ldots, \text{NL} \tag{14}$$

e. FACTS device constraints

TCSC reactance constraints: TCSC reactance must be restricted within their maximum and minimum limits as follows:

$$X_{\text{TCSC}_i}^{\min} \le X_{\text{TCSC}_i} \le X_{\text{TCSC}_i}^{\max}, \quad i = 1, \ldots, \text{NTCSC} \tag{15}$$

SVC reactive power constraints: SVC reactive power must be restricted within their maximum and minimum limits as follows:

$$Q_{\text{SVC}_i}^{\min} \le Q_{\text{SVC}_i} \le Q_{\text{SVC}_i}^{\max}, i = 1, \ldots, \text{NSVC} \tag{16}$$

2.1.3 Constraints Handling

The equality constraints are satisfied by running the Newton–Raphson power flow algorithm. The inequality constraints on the control variables are self-restricted between the minimum and maximum value by the optimization algorithm. The dependent variables which contain V_{L}, P_{G1}, Q_{G} and S_l must be penalized to be in the upper and lower limits. A quadratic penalty factor is added to the objective function F as follows (Abou El Ela and Abido 2010):

$$\begin{aligned} F(x,u) = F &+ \lambda_P \left(P_{\text{G}_1} - P_{\text{G}_1}^{\lim}\right)^2 \\ &+ \lambda_V \sum_{i=1}^{\text{NL}} \left(V_{L_i} - V_{L_i}^{\lim}\right)^2 \\ &+ \lambda_Q \sum_{i=1}^{\text{NG}} \left(Q_{\text{G}i} - Q_{\text{G}_1}^{\lim}\right)^2 \\ &+ \lambda_S \sum_{i=0}^{nl} \left(S_{l_i} - S_{l_i}^{\lim}\right)^2 \end{aligned} \tag{17}$$

where λ_P, λ_V, λ_Q and λ_S are penalty factors and $x^{\lim}$ is the limit value of the dependent variable x and given as:

$$x^{\lim} = \begin{cases} x; & x^{\min} \le x \le x^{\max} \\ x^{\max}; & x > x^{\max} \\ x^{\min}; & x < x^{\min} \end{cases} \tag{18}$$

2.2 The Objective Functions

2.2.1 Case 1 Minimization of Fuel Cost

The main objective of OPF problem is to minimize the total fuel cost of power plants. The objective function F represents the total production cost in the system, and it may be expressed as a quadratic function of the active power outputs from the generating units. Mathematically, the generation fuel cost can be written as follows:

$$F = \sum_{i=1}^{\text{NG}} f_i = \sum_{i=1}^{\text{NG}} a_i + b_i P_{G_i} + c_i P_{G_i}^2 \ (\$/\text{h}) \tag{19}$$

f_i is the expression for cost function corresponding to ith generating unit, and a_i, b_i and c_i are the cost coefficients of the i-th generator.

2.2.2 Case 2 Minimization of Voltage Magnitude Deviation

Bus voltage is considered as one of the most important security and service quality indices (Abido 2002a). Minimizing only a cost-based objective in an OPF problem may give non-feasible values in voltage profile. Therefore, an additional voltage magnitude deviation function is considered with fuel cost function in this case. The goal is to reduce the fuel cost

and increase voltage profile simultaneously by keeping the PQ bus voltage values close to 1.0 per unit. The objective function can be expressed as

$$F = F_{\text{cost}} + w.F_{\text{Voltage_deviation}} \tag{20}$$

where w is an appropriate weighting factor. The latter must be selected carefully to give a balance between the two objective functions. F_{cost} and $F_{\text{Voltage_deviation}}$ are specified as follows (Bouchekara et al. 2014):

$$F_{\text{cost}} = \sum_{i=1}^{\text{NG}} f_i \tag{21}$$

$$F_{\text{Voltage_deviation}} = \sum_{i \in \text{NL}} |V_i - 1| \tag{22}$$

2.2.3 Case 3 Voltage Stability Enhancement

Power system stability is the ability of an electric power system, to conserve constantly acceptable bus voltage at each node under normal operating conditions, and after being subjected to a disturbance. On the other hand, a system enters a state of voltage instability when a disturbance causes a progressive and uncontrollable decline in voltage. The result would be the occurrence of voltage collapse which leads to total blackout of the whole system (Kundur et al. 2004; Zeng and Sun 2014).

Kessel and Glavitsch (1986) have developed an index called voltage stability indicator L-index. This index is an approximate measure of closeness of each bus in the system to voltage collapse. Generally, the value of L-index varies between zero and one corresponding to no-load condition and voltage collapse, respectively (Devaraj 2007).

Enhancing voltage stability can be achieved through minimizing the voltage stability indicator L-index values at every bus of the system; the L-index expression is given as follows (Bouchekara et al. 2014; Niknam et al. 2012a).

Consider an N-bus system, in which there are NG generators, and the network equations in terms of the node admittance matrix can be simply written as

$$I_{\text{bus}} = Y_{\text{bus}} \cdot V_{\text{bus}} \tag{23}$$

We can separate buses into two parts: PV buses at the head and PQ buses at the tail as follows

$$\begin{bmatrix} I_{\text{L}} \\ I_{\text{G}} \end{bmatrix} = [Y_{\text{bus}}] \begin{bmatrix} V_{\text{L}} \\ V_{\text{G}} \end{bmatrix} = \begin{bmatrix} Y_{\text{LL}} & Y_{\text{LG}} \\ Y_{\text{GL}} & Y_{\text{GG}} \end{bmatrix} \begin{bmatrix} V_{\text{L}} \\ V_{\text{G}} \end{bmatrix} \tag{24}$$

where Y_{LL}, Y_{LG}, Y_{GL} and Y_{GG} are submatrixes of Y_{bus}. I_{G}, I_{L}, V_{G} and V_{L} represent currents and voltages of PV buses and PQ buses, respectively.

Here, it is important to note that the presence of FACTS devices has a direct effect on the admittance matrix. Therefore, inclusion of TCSC in lines modifies reactance of that line and the admittance matrix is modified accordingly. Here, admittance matrix is modified with the new value of line reactance considering the presence of TCSC in that line (Bhattacharyya and Gupta 2014).

Similarly, the function of SVC is either to inject or to absorb reactive power to/from the bus where it is connected and modifies susceptance of that line and the admittance matrix is modified accordingly. So, the Ybus matrix will also be modified in the presence of SVC device. More details and discussion will be given in the following sections.

The last equations can be written as:

$$\begin{bmatrix} V_{\text{L}} \\ I_{\text{G}} \end{bmatrix} = [H] \begin{bmatrix} I_{\text{L}} \\ V_{\text{G}} \end{bmatrix} = \begin{bmatrix} H_{\text{LL}} & H_{\text{LG}} \\ H_{\text{GL}} & H_{\text{GG}} \end{bmatrix} \begin{bmatrix} I_{\text{L}} \\ V_{\text{G}} \end{bmatrix} \tag{25}$$

where H matrix is generated by the partial inversion of Y_{bus}, and H_{LL}, H_{LG}, H_{GL} and H_{GG} are submatrixes of H, which is given by:

$$[H] = \begin{bmatrix} Z_{\text{LL}} & -Z_{\text{LL}}Y_{\text{LG}} \\ Y_{\text{GL}}Z_{\text{LL}} & Y_{\text{GG}} - Y_{\text{GL}}Z_{\text{LL}}Y_{\text{LG}} \end{bmatrix}, Z_{\text{LL}} = Y_{\text{LL}}^{-1} \tag{26}$$

Consequently, the L-index of the j-th node is given by the expression,

$$L_j = \left| 1 - \sum_{i=1}^{\text{NG}} H_{\text{LG}_{ji}} \frac{V_i}{V_j} \right|, \quad j = 1, 2 \ldots, \text{NL} \tag{27}$$

For stable system, the condition $L \leq 1$ must not be violated for any of the buses j and more the value of L-index less than one more the system far from the voltage collapse point.

Hence, a global stability indicator (L_{max}) for the whole system can be expressed as:

$$L_{\max} = \max\left(L_j\right), \quad j = 1, 2 \ldots, \text{NL} \tag{28}$$

The situation of system is more stable as the value of $L_{\max}$ is lower.

In this case, the goal is to minimize the fuel cost and increase voltage stability simultaneously. Hence, the chosen objective function can be formulated by the following equation:

$$F = F_{\text{cost}} + w.F_{\text{Voltage_stability_enhancement}} \tag{29}$$

$$F_{\text{cost}} = \sum_{i=1}^{\text{NG}} f_i \tag{30}$$

$$F_{\text{Voltage_stability_enhancement}} = L_{\max} \tag{31}$$

where w is an appropriate weighting factor.

2.2.4 Case 4 Minimization of Real Power Losses

The main objective function of this case is to minimize the total active power losses in the transmission system. The objective function is given as (Bouchekara 2014):

$$F = \sum_{i=1}^{NB} P_i = \sum_{i=1}^{NB} P_{Gi} - \sum_{i=1}^{NB} P_{Di} \tag{32}$$

2.2.5 Case 5 Minimization of Reactive Power Losses

In this case the aim is to optimize reactive power losses by the minimization of the following equation (Bouchekara 2014):

$$F = \sum_{i=1}^{NB} Q_i = \sum_{i=1}^{NB} Q_{Gi} - \sum_{i=1}^{NB} Q_{Di} \tag{33}$$

3 Modeling of FACTS Devices

3.1 Modeling of TCSC

TCSC is a series compensator which consists of a thyristor-controlled reactor connected in parallel with a capacitive bank as presented in Fig. 1a; TCSC can be considered as controllable reactance inserted in series to related transmission line, and its principle is to increase or decrease the transmission line reactance in order to control power flow, reduce overload and enhance system loadability (Benabid et al. 2009; Gupta et al. 2014). In this paper, TCSC controllable reactance is directly used as the control variable in the power flow equations.

After installing TCSC, the equivalent reactance of line is defined as (Amrane et al. 2014):

$$x_{ij} = x_{ij}^{\text{line}} + x_{ij}^{\text{TCSC}} \tag{34}$$

where x_{ij}^{line} is the transmission line reactance, and x_{ij}^{TCSC} is the TCSC reactance, and the latter varies between the following limits,

$$-0.8x_{ij}^{\text{line}} \leq x_{ij}^{\text{TCSC}} \leq 0.2x_{ij}^{\text{line}} \tag{35}$$

The new admittance of the branch can be written as (Gupta et al. 2014)

$$Y_{ij} = \frac{1}{(r_{ij}^{\text{line}} + j(x_{ij}^{\text{line}} + x_{ij}^{\text{TCSC}}))} \tag{36}$$

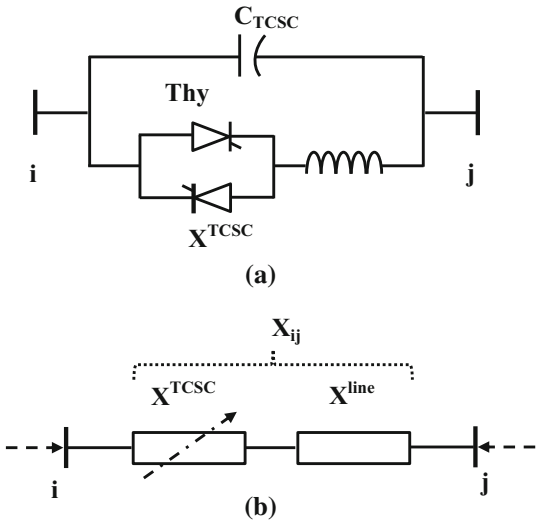


Fig. 1 TCSC: **a** basic structure, **b** model

where Y_{ij} is the bus admittance matrix with TCSC. r_{ij}^{line} is the transmission line resistance.

The static model of the network with TCSC connected between buses i and j is shown in Fig. 1b.

3.2 Modeling of SVC

The SVC is a shunt-connected VAR compensator. Like the TCSC, the SVC combines a series capacitor bank shunted by thyristor-controlled reactor (Fig. 2a). SVC is capable of controlling voltage magnitude by its ability to exchange dynamically reactive power (absorb or generate) with the specified connected bus of the network (Jothi Swaroopan and Somasundaram 2010; Hingorani and Gyugyi 1999). In this paper, the SVC is modeled as a variable shunt reactive susceptance, and Fig. 2b shows the SVC susceptance model representation. The reactive power provided is limited as (Amrane et al. 2014; Berrouk et al. 2014):

$$Q_{\text{SVC}} = -V_i^2 \times B_{\text{SVC}} \tag{37}$$

$$B_{\text{SVC}}^{\min} \leq B_{\text{SVC}} \leq B_{\text{SVC}}^{\max} \tag{38}$$

where Q_{SVC} is the SVC reactive power, and B_{SVC} is the SVC shunt susceptance.

4 The Proposed Hybrid Algorithm

4.1 Particle Swarm Optimization

Particle swarm optimization (PSO) is a population-based swarm intelligence method, originally introduced in terms

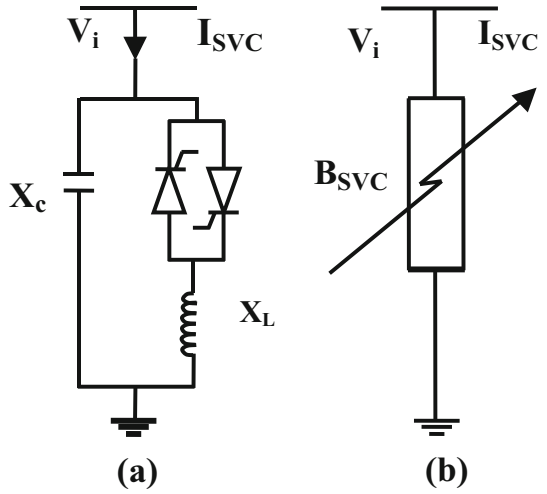


Fig. 2 SVC: **a** basic structure, **b** variable susceptance model

of social and cognitive behavior by Kennedy and Eberhart (1995). Due to the simple concepts and the ease of implementation, it has been successfully applied to a number of combinatorial optimization problems (Sahu et al. 2015).

In PSO, individuals are known as particles and the population is known as swarm. Each particle has a position and flies around in a multi-dimensional search space with some velocity. During flight, each particle adjusts its position according to its own experience (the best local position pbest), and the experience of neighboring particles (the best global position gbest), making use of the best position encountered by itself and its neighbors.

After each iteration, the pbest and gbest are updated for each particle if, in terms of fitness, a better solution is found. This process continues, iteratively, until the desired result is converged upon (Abido 2002a; Niknam et al. 2012b).

For an n-dimensional search space, at iteration (t) each particle (i) has its position defined by $X_i(t) = [X_{i,1}(t), X_{i,2}(t) \ldots X_{i,\mathrm{NP}}(t)]$ and velocity defined as $V_i(t) = [V_{i,1}(t), V_{i,2}(t) \ldots V_{i,\mathrm{NP}}(t)]$. Velocity and position of each particle in the next iteration can be calculated as

$$V_i\,(t+1) = w.V_i\,(t) + C_1 \cdot \mathrm{rand}_1\,(t) \cdot \left(\mathrm{pbest}_i(t) - X_i(t)\right) + C_2 \cdot \mathrm{rand}_2\,(t) \cdot \left(\mathrm{gbest}_i(t) - X_i(t)\right) \quad (39)$$

$$X_i\,(t+1) = X_i\,(t) + V_i\,(t+1) \quad , i = 1, 2 \ldots, \mathrm{NP} \quad (40)$$

where V_i and X_i are, respectively, the velocity and position of particle (i) at iteration $(t+1)$. w is the inertia weight factor, C_1 and C_2 are acceleration constants, rand_1 and rand_2 are random numbers selected between 0 and 1, and NP is number of particles.

The selection of w provides a balance between global and local explorations. In general, the inertia weight w is set as

$$w = w_{\max} - \frac{w_{\max} - w_{\min}}{\mathrm{Iter}_{\max}} \times \mathrm{iter} \quad (41)$$

where $\mathrm{Iter}_{\max}$ is the maximum number of iterations or generations and $w_{\max}$ and $w_{\min}$ are the upper and lower limits of the inertia weight.

4.2 Pattern Search Approach

The pattern search (PS) optimization technique is a simple effective evolutionary algorithm suitable to solve a variety of optimization problems related to power system domain. Comparatively with other heuristic method such as GA and PSO, PS has the advantage of being very simple in concept, easy to implement and computationally competitive. Furthermore, the PS has a unique feature, which is the ability to enhance and adapt the global and fine-tune local search by its flexible and balanced operator (Labbi and Attous 2014; Gabbar et al. 2016). The flowchart of the PS method can be seen in Fig. 3. A detail discussion of direct search methods for unconstrained optimization methods can be found in (Mahdad and Srairi 2014; Al-Sumait et al. 2007).

The pattern search operations can be summarized in the following steps:

1. The algorithm starts by establishing a set of points called mesh, and around the initial points ($X0$), these initial points or starting points are, either, provided by the user or it could be computed from the previous step of the algorithm (Mahdad and Srairi 2014; Panda et al. 2015).
2. At the first iteration, with a scalar = 1 called mesh size, the pattern or direction vectors are formed as [0 1], [1 0], [−1 0] and [0 −1]. Then, the mesh points are constructed by the addition of direction vectors to initial points ($X0$) as: $X0$ + [0 1], $X0$ + [1 0], $X0$ + [−1 0] and $X0$ + [0 −1].
3. The algorithm computes the objective function at all points in the mesh until it finds one whose value is smaller than the objective function value of $X0$.
4. If there is such point, the following happens:
   - 4.1 The minimum points found become the current points $X1$.
   - 4.2 The method multiplies the current mesh size by 2.
   - 4.3 The algorithm steps to the next iteration.
5. The value $X2$ will be defined if a value smaller than $X1$ is found and iterations continue.
6. If in a particular iteration, none of the mesh points has a smaller objective function value than initial/current points, in this case the following happens:
   - 6.1 The algorithm does not change the current points at the next iteration.
   - 6.2 The method multiplies the current mesh size by 0.5.

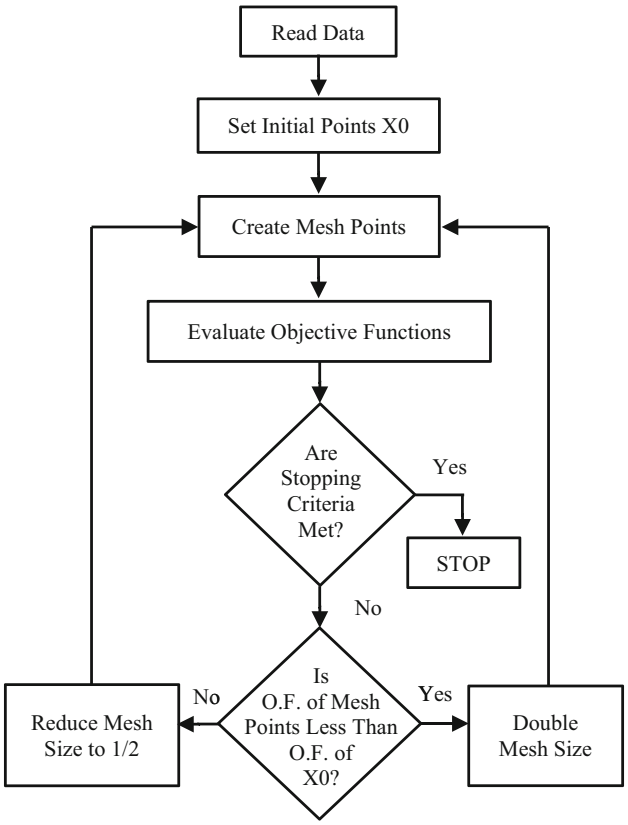


Fig. 3 Flowchart of pattern search (PS) algorithm

6.3 The algorithm steps to the next iteration.

7. The steps are repeated until any of the following stopping criteria is met:

7.1 The mesh size is less than mesh tolerance.
7.2 The algorithm reaches the value of max iteration.
7.3 The total number of objective function evaluations performed by the algorithm reaches the value of max function evaluations.
7.4 The change in the value of the objective function is less than X tolerance.

4.3 Hybrid Particle Swarm Optimization and Pattern Search Approach

The main objective of the proposed PSO-PS technique is to enhance the global search property of PSO by a robustness local search of PS. The principal is to merge the advantages of both PSO in exploitation and PS in exploration. In processes search, the best obtained solution of PSO algorithm (gbest) is used by the PS algorithm as an initial search points ($X0$) in aim to exploit and enforce the search around these points and improve the solution quality, and then the best obtained solution of PS algorithm is given to PSO as an initial solution.

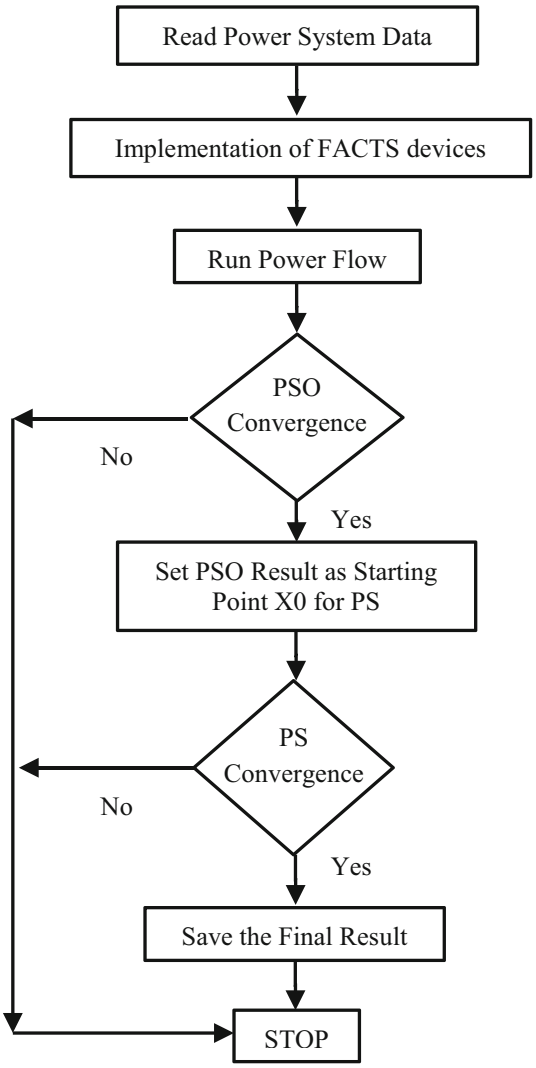


Fig. 4 Flowchart of the proposed PSO-PS method

This processes search is repeated until a stopping criterion is reached (Sahu et al. 2015; Niharika et al. 2016).

4.4 Stopping Criterion

Here, it is important to note that termination criterion of the hybrid PSO-PS algorithm is both the maximum number of iterations for the PSO algorithm and any of the stopping criteria for the PS algorithm mentioned above. A flowchart of the proposed hybrid PSO-PS algorithm is illustrated in Fig. 4.

5 Case Studies and Results

In the present paper, the proposed PSO-PS algorithm is applied to modified IEEE 30-bus test system with FACTS devices installed at fixed location for solving the OPF prob-

Table 1 Simulation parameters

PSO	Parameters	PS	Parameters
Population size	100	Mesh size	1
Number of generation	500	Number of generation	150
w_{max}	0.9	Mesh expansion factor	2
w_{min}	0.4	Mesh contraction factor	0.5
C1, C2	2		

Table 2 FACTS devices location

FACTS devices	Best location
TCSC	Branch: 28–27 (Line 36)
SVC	Bus: 22

lem. Table 1 shows the parameters of this algorithm. The optimal location of series and shunt FACTS devices is taken from (Benabid et al. 2009) and is given in Table 2. Further, the impact of the FACTS devices on cost, voltage deviation, voltage stability, real and reactive power losses is studied in this work.

The written algorithm is developed in MATLAB R2009b programming language, and the simulation is run on 2.67 GHz i5 PC with 4 GB RAM. Description on the test system and simulation results is presented.

5.1 IEEE 30-Bus Test System

The effectiveness of the proposed approach is tested on IEEE 30-bus test systems. This system has 6 generators located at buses: 1, 2, 5, 8, 11 and 13, 24 load buses, 41 transmission lines, 4 tap changing transformers at lines: 6–9, 6–10, 4–12 and 28–27, and 9 shunt capacitors at buses: 10, 12, 15, 17, 20, 21, 23, 24 and 29. The total system active and reactive loads demand at 100 MVA base is 283.4 MW and 126.2 MVAR, respectively. The test system is shown in Fig. 5. The branch parameters and loads are taken from MATPOWER package (Zimmerman et al. 2011). The generator data and cost coefficients can be found in (Mahdad et al. 2010) and are given in Table 3.

The upper and lower limits of the generator bus voltage, tap transformers, shunt capacitors and FACTS devices are summarized in Table 4. The voltage magnitude limits of loads buses are [0.95, 1.1 p.u.].

5.1.1 Case 1 Minimization of Fuel Cost

The objective of this case is the minimization of fuel cost for all generators. The obtained optimum control variables

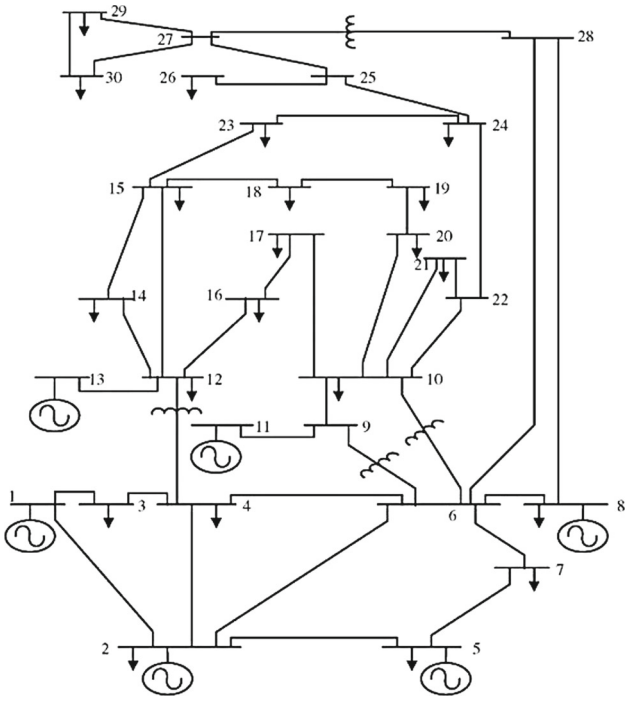


Fig. 5 IEEE 30-bus test system

Table 3 Generator (Gen) and cost coefficients data for IEEE 30-bus

Gen	P_{min}	P_{max}	Q_{min}	Q_{max}	Cost coefficients		
					a	b	c
G_1	50	200	− 20	250	0	2.00	0.00375
G_2	20	80	− 20	100	0	1.75	0.01750
G_5	15	50	− 15	80	0	1.00	0.06250
G_8	10	35	− 15	60	0	3.25	0.00834
G_{11}	10	30	− 10	50	0	3.00	0.02500
G_{13}	12	40	− 15	60	0	3.00	0.02500

Table 4 Setting of control variables

Variable	Min.	Max.
V_G (p.u.)	0.95	1.10
T (p.u.)	0.90	1.10
Q_{GC} (p.u.)	0	5
X_{TCSC} (p.u.)	$-0.8\ X_{line}$	$+0.2\ X_{line}$
Q_{SVC} (MVAr)	− 110	+ 80

from PSO and hybrid PSO-PS in the absence and presence of FACTS devices are listed in Table 5. The letter depicts the results of minimum generation cost, voltage deviation, stability index and power losses. The results are in their secure values and are far from the min. and max. limits. It can be seen from Table 5 that the obtained minimum cost is improved from 799.9738 $/h using PSO to 799.8723 $/h using PSO-PS and the best cost 799.5485 is given with inclu-

Table 5 Optimal control variable settings for minimization of fuel cost case

Control variable	PSO	PSO-PS	PSO-PS with FACTS
P_{G1} (MW)	178.1960	177.1504	177.0989
P_{G2}	48.9732	48.7208	48.7088
P_{G5}	21.3932	21.3146	21.3093
P_{G8}	21.7776	21.1636	21.1228
P_{G11}	10.0000	11.9056	11.9211
P_{G13}	12.0000	12.0000	12.0000
V_{G1} (p.u.)	1.1000	1.1000	1.1000
V_{G2}	1.0879	1.0879	1.0878
V_{G5}	1.0615	1.0616	1.0616
V_{G8}	1.0696	1.0697	1.0694
V_{G11}	1.1000	1.1000	1.1000
V_{G13}	1.1000	1.1000	1.1000
$T_{11(6-9)}$	1.0468	1.0465	1.0668
$T_{12(6-10)}$	0.9000	0.9000	0.9000
$T_{15(4-12)}$	1.0348	1.0343	1.0024
$T_{36(28-27)}$	0.9747	0.9746	0.9674
QC_{10}	0	0	0
QC_{12}	0	0	0
QC_{15}	0	0	0
QC_{17}	0	0	0
QC_{20}	0	0	0
QC_{21}	0	0	0
QC_{23}	0	0	0
QC_{24}	0	0	0
QC_{29}	0	0	0
X_{TCSC}	–	–	0.3131
Q_{SVC}	–	–	18.1168
Cost ($/h)	**799.9738**	**799.8723**	**799.5485**
VD (p.u.)	1.1290	1.1356	1.4590
L_{max} (p.u.)	0.1342	0.1342	0.1214
Ploss (MW)	8.9411	8.8560	8.7618
Qloss (MVar)	−0.4668	−0.8589	−2.1629

Best objective function values are given in bold

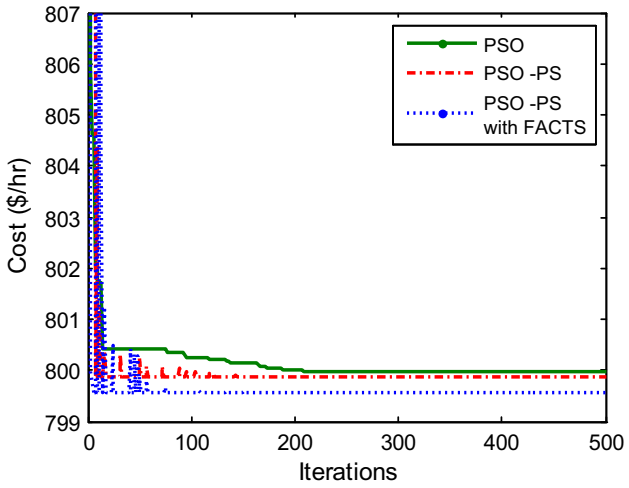


Fig. 6 Fuel cost variations with different proposed approaches

Table 6 Comparison of results for minimization of fuel cost case

Method	Cost ($/h)	References
PSO-PS with FACTS	**799.5485**	–
EGA-DQLF	799.56	Kumari and Maheswarapu (2010)
PSO-PS	**799.8723**	–
BHBO	799.9217	Bouchekara (2014)
EM	800.078	Bouchekara (2016)
EEA	800.0831	Surender Reddy et al. (2014)
DSA	800.3887	Abaci and Yamacli (2016)
EPGA	800.9617	Mahdad et al. (2010)
SOS	801.5733	Duman (2016)
AGSO	801.75	Daryani et al. (2016)
GA-PSO	801.81	Roselyn et al. (2011)
PSO-SA	801.96	Niknam et al. (2012b)
TS	802.29	Abido (2002b)
GA	803.699	Bouktir et al. (2004)
SA	805.45	Roa-Sepulveda and Pavez-Lazo (2003)

Best objective function values are given in bold

sion of FACTS devices. Here, it is important to note that FACTS devices can decrease the total fuel cost in power system. In this case, the total voltage deviation in the presence of FACTS is 1.4590 p.u. The corresponding total active and reactive power losses and voltage stability index are: 8.7618 MW, −2.1629 MVar and 0.1214 p.u., respectively. The comparative convergence characteristics of minimum fuel cost with proposed approaches are shown in Fig. 6. In addition, obtained results are compared with other methods reported in the literature and all these results are summarized in Table 6. It is clearly seen that proposed PSO-PS is better solution than other methods.

5.1.2 Case 2 Minimization of Voltage Magnitude Deviation

The optimized control variables and objective function value results obtained using PSO-PS with and without FACTS devices for this case are presented in Table 7 and compared with other methods such as BHBO and EM (Bouchekara 2014, 2016) in Table 8. The convergence curve of voltage deviation results over the iterations for different approaches is shown in Fig. 7. The variation of fuel cost and voltage deviation for the PSO-PS algorithm in the presence of FACTS devices is shown in Fig. 8. It can be seen from Table 7 that

Table 7 Optimal control variable settings for voltage profile improvement case

Control variable	PSO	PSO-PS	PSO-PS with FACTS
P_{G1} (MW)	184.8192	176.5139	176.0196
P_{G2}	50.9818	48.8777	48.8563
P_{G5}	22.3303	21.8114	21.6847
P_{G8}	10.0000	22.2434	22.5944
P_{G11}	13.9845	11.8459	12.2361
P_{G13}	12.0000	12.0000	12.0000
V_{G1} (p.u.)	1.0414	1.0365	1.0320
V_{G2}	1.0243	1.0214	1.0153
V_{G5}	1.0153	1.0116	1.0146
V_{G8}	1.0013	0.9996	1.0001
V_{G11}	1.0758	1.0789	1.0532
V_{G13}	0.9865	0.9938	1.0070
$T_{11(6-9)}$	1.1000	1.1000	1.0689
$T_{12(6-10)}$	0.9000	0.9000	0.9108
$T_{15(4-12)}$	0.9422	0.9535	0.9717
$T_{36(28-27)}$	0.9475	0.9654	0.9661
QC_{10}	0	3.6696	0
QC_{12}	0	2.4767	0.3305
QC_{15}	5.0000	5.0000	4.9998
QC_{17}	5.0000	0	0.9336
QC_{20}	5.0000	5.0000	5.0000
QC_{21}	5.0000	5.0000	0.1169
QC_{23}	5.0000	4.9991	4.7983
QC_{24}	5.0000	5.0000	5.0000
QC_{29}	0	2.2510	3.0904
X_{TCSC}	–	–	0.6036
Q_{SVC}	–	–	10.2256
Cost ($/h)	**805.7064**	**803.8194**	**804.3092**
VD (p.u.)	**0.1043**	**0.0984**	**0.0955**
L_{max} (p.u.)	0.1380	0.1369	0.1451
Ploss (MW)	10.7132	9.8899	9.9887
Qloss (MVar)	11.2352	8.7207	7.7490

Best objective function values are given in bold

Table 8 Comparisons of results for voltage profile improvement case

Method	Voltage deviation (p.u.)	References
PSO-PS with FACTS	**0.0955**	–
PSO-PS	**0.0984**	–
BHBO	0.1262	Bouchekara (2014)
EM	0.1270	Bouchekara (2016)

Best objective function values are given in bold

the obtained minimum voltage deviation is improved from 0.1043 p.u. using PSO to 0.0984 p.u. using PSO-PS and with the inclusion of FACTS devices, voltage deviation is reduced to 0.0955 p.u. It is worth mentioning in this case that FACTS

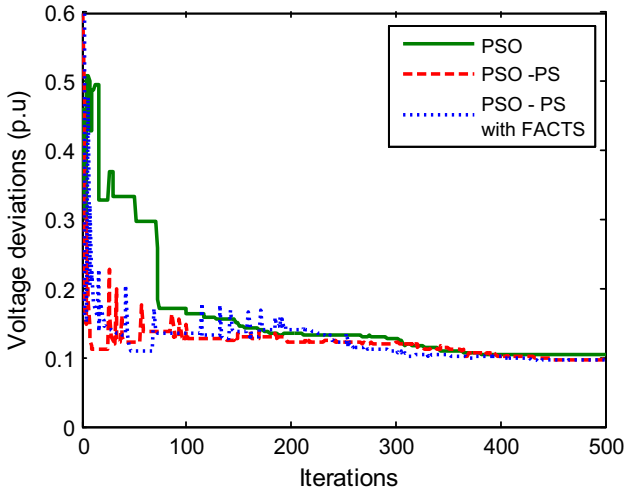


Fig. 7 Voltage deviation minimization with different proposed approaches

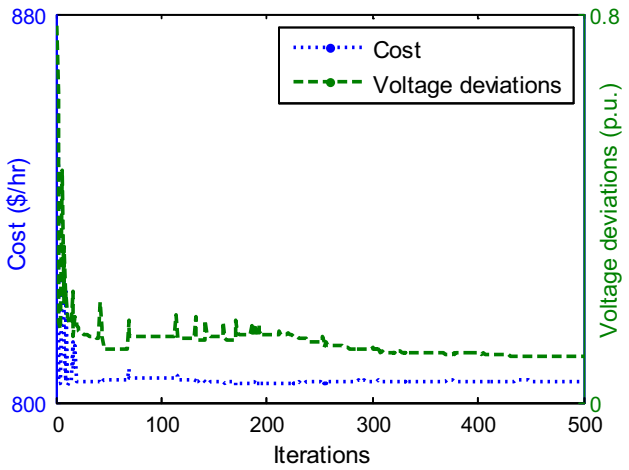


Fig. 8 Variations of fuel cost and voltage deviations for case 2

devices are very effective for the minimization of voltage deviation. Furthermore, the best voltage deviation offered by case 2 is greatly decreased compared to previous case, from 1.4590 p.u. in case 1 to 0.0955 p.u. in case 2 (% 93.45). Also, voltage magnitudes at all buses are within the security limits. The cost obtained in the presence of FACTS for this case is 804.3092, while L_{max}, Ploss and Qloss are 0.1451 p.u. 9.9887 MW and 7.7490 MVar, respectively. In addition, the optimized reactive power delivered by the SVC is 10.2256 MVAR, while X_{TCSC} is 0.6036 p.u. From Table 8, it is clear that the proposed approach gives better results than other methods.

5.1.3 Case 3 Voltage Stability Enhancement

The optimal values of control variables and objective functions for voltage stability enhancement objective are given

Table 9 Optimal control variable settings for voltage stability enhancement case

Control variable	PSO	PSO-PS	PSO-PS with FACTS
P_{G1} (MW)	178.6142	177.9429	176.2002
P_{G2}	49.0816	48.8522	48.5270
P_{G5}	21.6227	21.4009	21.2608
P_{G8}	21.7562	20.7931	20.9841
P_{G11}	10.0017	11.6061	13.2088
P_{G13}	12.0000	12.0000	12.0000
V_{G1} (p.u.)	1.0673	1.0834	1.1000
V_{G2}	1.0451	1.0600	1.0888
V_{G5}	1.0101	1.0288	1.0655
V_{G8}	1.0046	1.0300	1.0725
V_{G11}	1.1000	1.1000	1.1000
V_{G13}	1.1000	1.1000	1.1000
$T_{11(6-9)}$	0.9000	0.9000	1.0676
$T_{12(6-10)}$	1.1000	1.0960	0.9000
$T_{15(4-12)}$	0.9000	0.9255	0.9701
$T_{36(28-27)}$	0.9000	0.9225	1.0076
QC_{10}	5.0000	5.0000	5.0000
QC_{12}	5.0000	5.0000	5.0000
QC_{15}	5.0000	5.0000	4.9994
QC_{17}	5.0000	5.0000	5.0000
QC_{20}	5.0000	5.0000	0
QC_{21}	5.0000	5.0000	5.0000
QC_{23}	5.0000	5.0000	4.6159
QC_{24}	5.0000	5.0000	5.0000
QC_{29}	5.0000	5.0000	5.0000
X_{TCSC}	–	–	0
Q_{SVC}	–	–	22.4861
Cost ($/hr)	**802.5204**	**800.8754**	**799.9284**
VD (p.u.)	1.5366	1.7165	1.9420
L_{max} (p.u.)	**0.1156**	**0.1148**	**0.0758**
Ploss (MW)	9.6751	9.1944	8.7801
Qloss (MVar)	11.8665	5.9523	−3.9749

Best objective function values are given in bold

in Table 9. Here, it is important to confirm that all security constraints such as voltages at load buses and transmission line loading are satisfied and are within their admissible limits. The variation of stability index results with different proposed approaches during search process is represented in Fig. 9. A comparison of these results with different methods is shown in Table 10. The convergence curve of fuel cost and stability index for the PSO-PS algorithm in the presence of FACTS devices is shown in Fig. 10. From Table 9, the minimum total fuel cost and L_{max} found by the PSO-PS algorithm in the presence of FACTS are 799.9284 $/h and 0.0758 p.u., respectively, which show 37.56% reduction in the L_{max} and about 0.047% increase

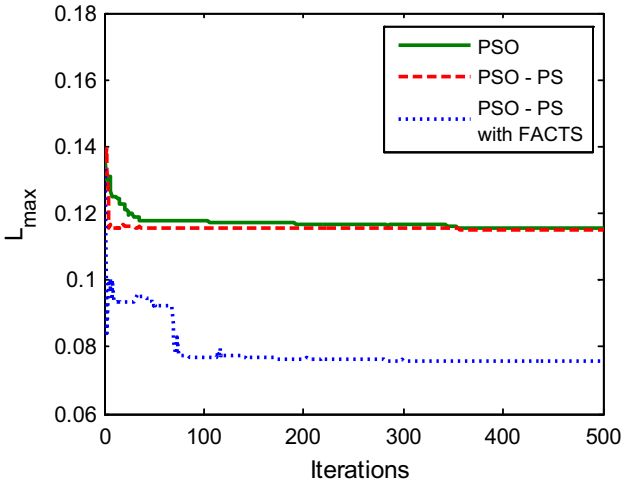


Fig. 9 Stability index minimization with different proposed approaches

Table 10 Comparison of results for voltage stability enhancement case

Method	L_max (p.u.)	References
PSO-PS with FACTS	**0.0758**	–
EGA-DQLF	0.10402	Kumari and Maheswarapu 2010
EEA	0.1052	Surender Reddy et al. (2014)
PSO-PS	**0.1148**	–
EM	0.1156	Bouchekara (2016)
BHBO	0.11671	Bouchekara (2014)
DSA	0.1244	Abaci and Yamacli (2016)

Best objective function values are given in bold

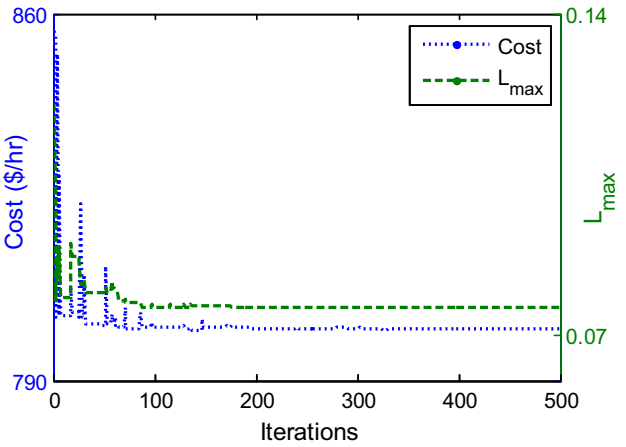


Fig. 10 Variations of fuel cost and stability index for case 3

in the total fuel cost in comparison with case 1 (cost: 799.5485 $/h, L_{max}: 0.1214 p.u.). Comparing the results in the absence and presence of FACTS devices, it is seen that introducing FACTS devices can greatly improve stabil-

ity index (33.97%), from 0.1148 to 0.0758 p.u. Moreover, these results are significantly decreased in comparison with case 1 (0.1214 p.u.) and case 2 (0.1451 p.u.). Additionally, the optimized reactive power delivered by the SVC for this case is 22.4861 MVAR, while real and reactive power losses are 8.7801 MW and −3.9749 MVar, respectively. Table 10 shows that the obtained result is the better in comparison with the other methods.

5.1.4 Case 4 Minimization of Real Power Losses

The optimal settings of control variables and objective functions using PSO, PSO-PS in the absence and presence of FACTS devices are listed in Table 11, and its convergence characteristic is shown in Fig. 11. Here, it is important to confirm that all control variables and state variables are within their security limits. It is seen from Table 11 that the optimal real losses value obtained by PSO-PS algorithm in the presence of FACTS device is 2.7914 MW which reduces by about 2.097% compared with the 2.8512 MW obtained by PSO-PS (without FACTS) and reduces by about 12.08% compared with the 3.1752 MW obtained by PSO, and this value is the best compared with different methods in the literature as shown in Table 12. In this case, the optimized reactive power delivered by the SVC is 5.9698 MVAR, while X_{TCSC}, L_{max} and Qloss are −0.2487, 0.0827 p.u. and −24.7175 MVar, respectively.

Table 11 Optimal control variable settings for real power losses case

Control variable	PSO	PSO-PS	PSO-PS with FACTS
P_{G1} (MW)	51.5757	51.2498	51.1920
P_{G2}	80.0000	80.0000	80.0000
P_{G5}	50.0000	50.0000	50.0000
P_{G8}	35.0000	35.0000	35.0000
P_{G11}	30.0000	30.0000	30.0000
P_{G13}	40.0000	40.0000	40.0000
V_{G1} (p.u.)	1.0331	1.1000	1.1000
V_{G2}	1.0281	1.0976	1.0976
V_{G5}	1.0067	1.0799	1.0799
V_{G8}	1.0129	1.0869	1.0868
V_{G11}	1.1000	1.1000	1.1000
V_{G13}	1.1000	1.1000	1.1000
$T_{11(6-9)}$	0.9000	1.0550	1.0690
$T_{12(6-10)}$	0.9000	0.9000	0.9000
$T_{15(4-12)}$	0.9331	0.9842	0.9841
$T_{36(28-27)}$	0.9136	0.9727	0.9824
QC_{10}	0	5.0000	5.0000
QC_{12}	5.0000	5.0000	5.0000
QC_{15}	5.0000	5.0000	5.0000
QC_{17}	5.0000	5.0000	5.0000
QC_{20}	0	5.0000	4.1859
QC_{21}	5.0000	5.0000	5.0000
QC_{23}	5.0000	3.5972	2.7385
QC_{24}	5.0000	5.0000	5.0000
QC_{29}	2.8784	2.5213	2.4170
X_{TCSC}	–	–	−0.2487
Q_{SVC}	–	–	5.9698
VD (p.u.)	1.5890	2.0503	2.0825
L_{max} (p.u.)	0.1195	0.1150	0.0827
Ploss (MW)	**3.1752**	**2.8512**	**2.7914**
Qloss (MVar)	−9.6319	−24.3696	−24.7175

Best objective function values are given in bold

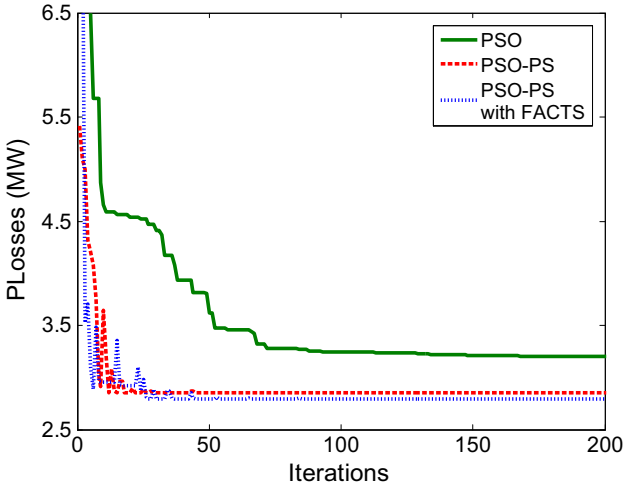


Fig. 11 Real power losses minimization with different proposed approaches

Table 12 Comparison of results for real power loss minimization

Method	Real power losses (MW)	References
PSO-PS with FACTS	**2.7914**	–
PSO-PS	**2.8512**	–
DSA	3.0945	Abaci and Yamacli (2016)
EM	3.1775	Bouchekara (2016)
EGA-DQLF	3.2008	Kumari and Maheswarapu (2010)
EEA	3.2823	Surender Reddy et al. (2014)
BHBO	3.5035	Bouchekara (2014)

Best objective function values are given in bold

5.1.5 Case 5 Minimization of Reactive Power Losses

In this case, the optimal settings of control variables and objective functions are given in Table 13. It is seen from

Table 13 Optimal control variable settings for reactive power losses case

Control variable	PSO	PSO-PS	PSO-PS with FACTS
P_{G1} (MW)	51.4581	51.3087	51.2577
P_{G2}	80.0000	80.0000	80.0000
P_{G5}	50.0000	50.0000	50.0000
P_{G8}	35.0000	35.0000	35.0000
P_{G11}	30.0000	30.0000	30.0000
P_{G13}	40.0000	40.0000	40.0000
V_{G1} (p.u.)	1.1000	1.1000	1.1000
V_{G2}	1.1000	1.1000	1.1000
V_{G5}	1.0920	1.0920	1.0921
V_{G8}	1.1000	1.1000	1.1000
V_{G11}	1.1000	1.1000	1.1000
V_{G13}	1.1000	1.1000	1.1000
$T_{11(6-9)}$	0.9650	1.0016	1.0004
$T_{12(6-10)}$	1.1000	0.9660	1.0034
$T_{15(4-12)}$	0.9757	0.9948	0.9941
$T_{36(28-27)}$	0.9796	0.9861	0.9983
QC_{10}	0	5.0000	5.0000
QC_{12}	5.0000	5.0000	5.0000
QC_{15}	0	5.0000	5.0000
QC_{17}	5.0000	5.0000	5.0000
QC_{20}	5.0000	5.0000	5.0000
QC_{21}	0	5.0000	5.0000
QC_{23}	5.0000	5.0000	3.9636
QC_{24}	5.0000	5.0000	5.0000
QC_{29}	4.0341	3.2714	3.4325
X_{TCSC}	–	–	0
Q_{SVC}	–	–	9.8566
VD (p.u.)	1.8736	2.1318	2.1679
L_{max} (p.u.)	0.117	0.1142	0.0770
Ploss (MW)	3.0571	2.9102	2.8590
Qloss (MVar)	**−24.1499**	**−25.2040**	**−26.0946**

Best objective function values are given in bold

Table 11 that the best reactive losses value obtained by PSO-PS algorithm in the presence of FACTS device is −26.0946 MVar which reduces by about 3.41% compared with the −25.2040 MVar obtained by PSO-PS (without FACTS) and reduces by about 7.45% compared with the −24.1499 MVar obtained by PSO and is smaller than the values obtained by all previous cases. These results are better in comparison with results found from EM and BHBO methods as shown in Table 14. Additionally, the optimized reactive power delivered by the SVC in this case is 9.8566 MVAR, while L_{max} and Ploss are 0.0770 p.u. and 2.8590 MW, respectively. Finally, the variation of reactive power losses using PSO, PSO-PS with and without FACTS is sketched in Fig. 12.

Table 14 Comparison of results for reactive power losses minimization

Method	Reactive power losses (MVAR)	References
PSO-PS with FACTS	**−26.0946**	–
PSO-PS	**−25.204**	–
EM	−22.0196	Bouchekara (2016)
BHBO	−20.1522	Bouchekara (2014)

Best objective function values are given in bold

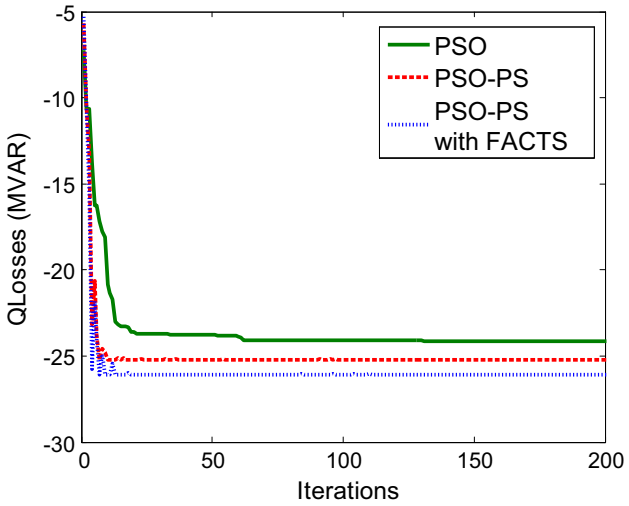


Fig. 12 Reactive power losses minimization with different proposed approaches

6 Conclusion

In this paper, hybrid particle swarm optimization (PSO) and pattern search (PS) algorithm has introduced, adapted and applied for the solution of optimal power flow problem of power system equipped with two different types of FACTS devices. The OPF problem has been formulated as a nonlinear optimization problem with equality and inequality constraints. Here, the proposed hybrid PSO-PS algorithm has been tested on IEEE 30-bus test system for different types of objective functions. This test system is equipped with SVC and TCSC devices at fixed locations. From the results, it is found that the combined use of both SVC and TCSC devices can effectively minimize the generation cost, enhance voltage deviation, decrease real and reactive losses and improve the voltage stability index in power system. The simulation results also demonstrate the effectiveness of the proposed PSO-PS algorithm to solve the OPF problem of power system equipped with FACTS devices. The results of the proposed algorithms have been compared with other recent methods reported in the literature, and the comparison confirms the superiority of the proposed method for all study cases in terms of solution quality. Finally, author will strive

to adapt and apply, as a future work, newest hybrid algorithms to solve multi-objective optimal power flow problem based on Pareto optimal solutions for large power system with inclusion of multi-FACTS devices such as SVC, TCSC, TCPS, SSSC, STATCOM and UPFC.

References

Abaci, K., & Yamacli, V. (2016). Differential search algorithm for solving multi-objective optimal power flow problem. *International Journal of Electrical Power and Energy Systems*, *79*, 1–10.

Abarghooeea, R. A., Narimania, M. R., Firouzia, B. B., & Niknamb, T. (2014). Modified shuffled frog leaping algorithm for multiobjective optimal power flow with FACTS devices. *Journal of Intelligent and Fuzzy Systems*, *26*, 681–692.

Abido, M. A. (2002a). Optimal power flow using particle swarm optimization. *International Journal of Electrical Power and Energy Systems*, *24*, 563–571.

Abido, M. A. (2002b). Optimal power flow using Tabu search algorithm. *Electric Power Systems Research*, *30*, 469–483.

Abou El Ela, A. A., & Abido, M. A. (2010). Optimal power flow using differential evolution algorithm. *Electric Power Systems Research*, *80*, 878–885.

Al-Muhawesh, T. A., & Qamber, I. S. (2008). The established megawatt linear programming-based optimal power flow model applied to the real power 56-bus system in eastern province of Saudi Arabia. *Energy*, *33*, 12–21.

Al-Sumait, J. S., AL-Othman, A. K., & Sykulski, J. K. (2007). Application of pattern search method to power system valve-point economic load dispatch. *International Journal of Electrical Power and Energy Systems*, *29*, 720–730.

Amrane, Y., Boudour, M., & Belazzoug, M. (2014). A new hybrid technique for power systems multi-facts optimization design. *International Transactions on Electrical Energy Systems*, *25*, 2961–2981.

Ayan, K., Kılıç, U., & Baraklı, B. (2015). Chaotic artificial bee colony algorithm based solution of security and transient stability constrained optimal power flow. *International Journal of Electrical Power and Energy Systems*, *64*, 136–147.

Basu, M. (2011). Multi-objective optimal power flow with FACTS devices. *Energy Conversion and Management*, *52*, 903–910.

Benabid, R., Boudour, M., & Abido, M. A. (2009). Optimal location and setting of SVC and TCSC devices using non-dominated sorting particle swarm optimization. *International Journal of Electrical Power and Energy Systems*, *79*, 1668–1677.

Berrouk, F., Ali Rachedi, B., Lemzadmi, A., Bounaya, K., & Zeghache, H. (2014). Applications of Shunt FACTS controller for voltage stability improvement. In *Proceedings of the IEEE international conference on electrical sciences and technologies in Maghreb (CISTEM)*. https://doi.org/10.1109/CISTEM.2014.7077022.

Bhattacharyya, B., & Gupta, V. K. (2014). Fuzzy based evolutionary algorithm for reactive power optimization with FACTS devices. *International Journal of Electrical Power and Energy Systems*, *61*, 39–47.

Bouchekara, H. R. E. H. (2014). Optimal power flow using black-hole-based optimization approach. *Applied Soft Computing*, *24*, 879–888.

Bouchekara, H. R. E. H. (2016). Optimal power flow using electromagnetism-like mechanism. *Electric Power Components and Systems*, *44*, 1–16.

Bouchekara, H. R. E. H., Abido, M. A., & Boucherma, M. (2014). Optimal power flow using teaching–learning-based optimization technique. *Electric Power Systems Research*, *114*, 49–59.

Bouktir, T., Slimani, L., & Belkacemi, M. (2004). A genetic algorithm for solving the optimal power flow problem. *Leonardo Journal of Sciences*, *4*, 44–58.

Carpentier, J. (1962). Contribution to the economic dispatch problem. *Bulletin Society Francaise Electriciens*, *3*, 431–447.

Daryani, N., Hagh, M. T., & Teimourzadeh, S. (2016). Adaptive group search optimization algorithm for multi-objective optimal power flow problem. *Applied Soft Computing*, *38*, 1012–1024.

Devaraj, D. (2007). Improved genetic algorithm for multi-objective reactive power dispatch problem. *European Transactions on Electrical Power*, *17*, 569–581.

Dommel, H. W., & Tinney, W. F. (1968). Optimal power flow solutions. *IEEE Transactions on Power Apparatus and Systems*, *87*, 1866–1876.

Duman, S. (2016). Symbiotic organisms search algorithm for optimal power flow problem based on valve-point effect and prohibited zones. *Neural Computing and Applications*, *28*, 3571–3585.

Gabbar, H. A., Labbi, Y., Bower, L., & Pandya, D. (2016). Performance optimization of integrated gas and power within microgrids using hybrid PSO-PS algorithm. *International Journal of Energy Research*, *40*, 971–982.

Ghasemi, M., Ghavidel, S., Ghanbarian, M. M., Gharibzadeh, M., & Vahed, A. A. (2014a). Multi-objective optimal power flow considering the cost, emission, voltage deviation and power losses using multi-objective modified imperialist competitive algorithm. *Energy*, *78*, 276–289.

Ghasemi, M., Ghavidel, S., Rahmani, S., Roosta, A., & Falah, H. (2014b). A novel hybrid algorithm of imperialist competitive algorithm and teaching learning algorithm for optimal power flow problem with non-smooth cost functions. *Engineering Applications of Artificial Intelligence*, *29*, 54–69.

Gnanambal, K., & Babulal, C. K. (2012). Maximum loadability limit of power system using hybrid differential evolution with particle swarm optimization. *International Journal of Electrical Power and Energy Systems*, *43*, 150–155.

Gupta, V. K., Kumar, S., & Bhattacharyya, B. (2014). Enhancement of power system loadability with FACTS devices. *Journal of The Institution of Engineers (India): Series B*, *95*, 113–120.

Hingorani, N. G., & Gyugyi, L. (1999). Understanding FACTS. In *Concepts and technology of flexible AC transmission systems*. IEEE Computer Society Press.

Joorabian, M., & Afzalan, E. (2014). Optimal power flow under both normal and contingent operation conditions using the hybrid fuzzy particle swarm optimisation and Nelder–Mead algorithm (HFPSO–NM). *Applied Soft Computing*, *14*, 623–633.

Jothi Swaroopan, N. M., & Somasundaram, P. (2010). Fuzzified PSO Algorithm for OPF with FACTS Devices in interconnected Power Systems. In *Swarm and evolutionary computing conference (SEMCCO)*, LNCS, vol. 6466, 468–480.

Kennedy, J., & Eberhart, R. (1995). Particle swarm optimization. *IEEE International Conference on Neural Networks*, *4*, 1942–1948.

Kessel, P., & Glavitsch, H. (1986). Estimating the voltage stability of a power system. *IEEE Transactions on Power Delivery*, *1*, 346–354.

Kumari, M. S., & Maheswarapu, S. (2010). Enhanced genetic algorithm based computation technique for multi-objective optimal power flow solution. *International Journal of Electrical Power and Energy Systems*, *32*, 736–742.

Kundur, P., Paserba, J., Ajjarapu, V., Andersson, G., Bose, A., Canizares, C., et al. (2004). Definition and classification of power system stability IEEE/CIGRE joint task force on stability terms and definitions. *IEEE Transactions on Power Systems*, *19*, 1387–1401.

Labbi, Y., & Attous, D. B. (2014). A hybrid particle swarm optimization and pattern search method to solve the economic load dispatch problem. *International Journal of System Assurance Engineering and Management*, *5*, 435–443.

Mahdad, B., & Srairi, K. (2014). Multi objective large power system planning under sever loading condition using learning DE–APSO–PS strategy. *Energy Conversion and Management*, *87*, 338–350.

Mahdad, B., & Srairi, K. (2015). Blackout risk prevention in a smart grid based flexible optimal strategy using Grey Wolf-pattern search algorithms. *Energy Conversion and Management*, *98*, 411–429.

Mahdad, B., Srairi, K., & Bouktir, T. (2010). Optimal power flow for large-scale power system with shunt FACTS using efficient parallel GA. *International Journal of Electrical Power and Energy Systems*, *32*, 507–517.

Momoh, J. A., Guo, S. X., Ogbuobiri, E. C., & Adapa, R. (1994). The quadratic interior point method solving power system optimization problems. *IEEE Transactions on Power Systems*, *9*, 1327–1336.

Momoh, J. A., & Zhu, J. (1999). Improved interior point method for OPF problems. *IEEE Transactions on Power Systems*, *14*, 1114–1120.

Mukherjee, A., & Mukherjee, V. (2016). Solution of optimal power flow with FACTS devices using a novel oppositional krill herd algorithm. *International Journal of Electrical Power and Energy Systems*, *78*, 700–714.

Niharika, S., Rajesh. B., & Girish, P. (2016). Optimal LFC system of interconnected thermal power plants using hybrid particle swarm optimization-pattern search algorithm (hPSO-PS). In *IEEE 2nd international conference on communication, control and intelligent systems (CCIS)*. https://doi.org/10.1109/CCIntelS.2016.7878236.

Niknam, T., Narimani, M. R., Aghaei, J., & Azizipanah-Abarghooee, R. (2012a). Improved particle swarm optimization for multi-objective optimal power flow considering the cost, loss, emission and voltage stability index. *IET Generation, Transmission and Distribution*, *6*, 515–527.

Niknam, T., Narimani, M. R., & Jabbari, M. (2012b). Dynamic optimal power flow using hybrid particle swarm optimization and simulated annealing. *European Transactions on Electrical Power*, *23*, 975-01.

Niknam, T., Narimani, M. R., Jabbari, M., & Malekpour, A. R. (2011). A modified shuffle frog leaping algorithm for multi-objective optimal power flow. *Energy*, *36*, 6420–6432.

Ongsakul, W., & Bhasaputra, P. (2002). Optimal power flow with FACTS devices by hybrid TS/SA approach. *International Journal of Electrical Power and Energy Systems*, *24*, 851–857.

Panda, S., Kiran, S. H., Dash, S. S., & Subramani, C. (2015). A PD-type multi input single output SSSC damping controller design employing hybrid improved differential evolution-pattern search approach. *Accepted at Applied Soft Computing*, *32*, 532–543.

Roa-Sepulveda, C. A., & Pavez-Lazo, B. J. (2003). A solution to the optimal power flow using simulated annealing. *International Journal of Electrical Power and Energy Systems*, *25*, 47–57.

Roselyn, J. P., Devaraj, D., & Dash, S. (2011). Economic emission OPF using hybrid GA particle swarm optimization. In *Swarm and Evolutionary Computing Conference, LNCS*, vol. 7076, pp. 167–175.

Sahu, R. K., Panda, S., & Sekhar, G. T. C. (2015). A novel hybrid PSO-PS optimized fuzzy PI controller for AGC in multi area interconnected power systems. *International Journal of Electrical Power and Energy Systems, 64*, 880–893.

Singh, R. P., Mukherjee, V., & Ghoshal, S. P. (2016). Particle swarm optimization with an aging leader and challengers algorithm for the solution of optimal power flow problem. *Applied Soft Computing*, *40*, 161–177.

Sun, D. I., Ashley, B., Brewer, B., Hughes, A., & Tinney, W. F. (1984). Optimal power flow by Newton approach. *IEEE Transactions on Power Apparatus and Systems*, *103*, 2864–2875.

Surender Reddy, S., Bijwe, P. R., & Abhyankar, A. R. (2014). Faster evolutionary algorithm based optimal power flow using incremental variables. *International Journal of Electrical Power and Energy Systems*, *54*, 198–210.

Zeng, Y., & Sun, Y. (2014). Application of hybrid MOPSO algorithm to optimal reactive power dispatch problem considering voltage stability. *Journal of Electrical and Computer Engineering*, *2014*, 124136. https://doi.org/10.1155/2014/124136.

Zimmerman, R., Murillo-Sánchez, C., & Thomas, R. (2011). MATPOWER steady-state operations, planning and analysis tools for power systems research and education. *IEEE Transactions on Power Systems*, *26*, 12–19.